Wireless Pers Commun (2015) 84:999–1015
DOI 10.1007/s11277-015-2672-z

A Variable Diagonal Loading Beamformer with Joint Uncertainties of Steering Vector and Covariance Matrix

Jie Zhuang[1,2] · Tao Zhang[3] · Jing Chen[1] · Yulin Liu[4]

Published online: 15 May 2015

Abstract In this paper, a novel robust adaptive beamforming is proposed in which both the uncertainties of steering vector and covariance matrix are taken into account. First we develop a min–max optimization problem which aims to find a steering vector with the maximum output power under the worst-case covariance mismatch. Then we relax this min–max optimization problem to a max–min optimization problem which can be solved by using the Karush–Kuhn–Tucker optimality conditions. It is also shown that the proposed technique can be interpreted in terms of variable diagonal loading where the optimal loading factors are related to both the correlations (between the eigenvectors and the signal of interest) and the eigenvalues of the data covariance matrix. The effectiveness of the proposed approach is supported by computer simulation results.

Keywords Covariance matrix uncertainty · Robust adaptive beamforming (RAB) · Variable diagonal loading · Worst-case performance optimization

✉ Jie Zhuang
jz@uestc.edu.cn

Tao Zhang
zt361.love@163.com

Jing Chen
shance2675@gmail.com

Yulin Liu
spliuyl@uestc.edu.cn

1 School of Communication and Information Engineering (SCIE), University of Electronic Science and Technology of China (UESTC), Chengdu 611731, China

2 Chengdu Aerospace Communication Device Company, Chengdu, China

3 Sichuan XingBang Group Co. Ltd, Chengdu, China

4 China Electronic System Engineering Company, Shenyang 110005, China

1 Introduction

A ubiquitous task in array signal processing is adaptive beamforming which has been widely used in wireless communication, radar, sonar, acoustics, astronomy, medical imaging, and other areas [1, 2]. By means of adaptive beamforming, we can recover the signal of interest (SOI) in the presence of interferences and noise using an array of N sensors. Briefly stated, adaptive beamforming intends to estimate the temporal waveform $s(k)$ in the model

$$\begin{aligned} &\mathbf{x}(k) = \mathbf{a}_0 s(k) + \mathbf{i}(k) + \mathbf{n}(k) \\ &\text{with } \mathbf{i}(k) = \mathbf{A}_i \mathbf{u}(k) \end{aligned} \tag{1}$$

where $\mathbf{a}_0 \in \mathbb{C}^N$ stands for the steering vector (or signature) of the SOI, the matrix $\mathbf{A}_i = [\,\mathbf{a}_1 \quad \mathbf{a}_2 \quad \ldots \quad \mathbf{a}_M\,] \in \mathbb{C}^{N\times M}$ collects the steering vectors of M interferences, $\mathbf{u}(k) \in \mathbb{C}^M$ denotes the temporal waveforms of interferences, and $\mathbf{n}(k)$ represents the additive white Gaussian noise with power σ_n^2.

The second-order statistics of the $N \times 1$ signal-vector $\mathbf{x}(k)$ can be represented by the covariance matrix $\mathbf{R}$ as

$$\mathbf{R} = \mathcal{E}\{\mathbf{x}(k)\mathbf{x}^H(k)\} = \sigma_0^2 \mathbf{a}_0 \mathbf{a}_0^H + \sum_{m=1}^{M} \sigma_m^2 \mathbf{a}_m \mathbf{a}_m^H + \sigma_n^2 \mathbf{I} \tag{2}$$

where σ_0^2 and σ_m^2 respectively denote the powers of the SOI and the mth interference, and the matrix $\mathbf{I}$ stands for the identity matrix with proper size. The notations $\mathcal{E}\{\cdot\}$ and $(\cdot)^H$, respectively, denote the expectation operator and the Hermitian transpose. In practical applications, the theoretical covariance matrix in (2) is normally unavailable and we have to estimate it from the observations as follows:

$$\widehat{\mathbf{R}} = \frac{1}{K} \sum_{k=1}^{K} \mathbf{x}(k)\mathbf{x}^H(k) \tag{3}$$

where K is the snapshot number. Using the $N \times 1$ weight vector $\mathbf{w}$, the output of an adaptive beamformer is given by

$$\mathrm{y(k)} = \mathbf{w}^H \mathbf{x}(k).$$

The array output signal-to-interference-plus-noise ratio (SINR) is defined as

$$\mathrm{SINR} \triangleq \frac{\sigma_0^2 |\mathbf{w}^H \mathbf{a}_0|}{\mathbf{w}^H \mathbf{R}_{\mathrm{i+n}} \mathbf{w}} \tag{4}$$

where $\mathbf{R}_{\mathrm{i+n}} \triangleq \sum_{m=1}^{M} \sigma_m^2 \mathbf{a}_m \mathbf{a}_m^H + \sigma_n^2 \mathbf{I}$ is the interference-plus-noise covariance matrix.

The Capon beamformer is a representative example of an adaptive beamformer, in which the interferences and noise are suppressed as much as possible while the array response gain for the SOI keeps unchanged. More specifically, the Capon beamformer can be formulated by the following optimization problem

$$\begin{aligned} &\min_{\mathbf{w}} \ \mathbf{w}^H \mathbf{R} \mathbf{w} \\ &\quad \text{s.t. } \mathbf{w}^H \mathbf{a}_0 = 1 \end{aligned} \tag{5}$$

with the solution given by

$$\mathbf{w}_c = \frac{\mathbf{R}^{-1}\mathbf{a}_0}{\mathbf{a}_0^H\mathbf{R}^{-1}\mathbf{a}_0}. \tag{6}$$

The Capon beamformer performs well when the SOI steering vector $\mathbf{a}_0$ and the covariance matrix $\mathbf{R}$ are both obtained accurately. In practical applications, however, the traditional Capon beamformer may suffer substantial performance degradation in the presence of the mismatch between the nominal and the true SOI steering vector (or covariance matrix). The mismatch can include look direction errors, imperfect array calibration, source local scattering, wavefront distortions, etc. In such case, the SOI is likely to be treated as an interference and thus be suppressed, leading to "signal cancellation" Sometimes even a small mismatch may result in a severe performance degradation.

In the past decade, a number of robust adaptive beamforming (RAB) techniques have been reported to combat the effects of these mismatches for the Capon beamforming and therefore the RAB has been an intensive research topic in array signal processing. An excellent review and comparison of the existing robust techniques have been provided in [3, 4]; see also the references contained therein. Roughly speaking, these robust methods can be categorized into two main groups [5]: methods based on previous mismatch assumptions (such as [6–10]) and techniques that estimate the mismatch or equivalently the actual steering vector (such as [4, 11–17]). Among these approaches, the diagonal loading (DL) beamformer and its extension versions may be the most common.

While the majority of the literature focuses on the robustness against the mismatch in the steering vector, relatively few researchers have investigated possible RAB techniques with joint robustness against the uncertainties of both the covariance matrix and the steering vector. From (6), it is clear that the weight vector is a function of the covariance matrix and the SOI steering vector, which jointly affect the array output performance [18]. In many RAB methods, it is implicitly assumed that the uncertainty of the sample data covariance matrix can be incorporated into the steering vector uncertainty. As stated in [19], however, these two kinds of uncertainties are equivalent only under the condition when both the sample size (i.e., K) and the array input signal-to-noise (SNR) are large. Therefore, it is desired to design a RAB that is jointly robust against both the covariance matrix and the steering vector mismatches, which is referred to as joint RAB (JRAB) in this paper. To this end, some JRABs have been designed [18, 20, 21, 23]. The JRABs presented in [20, 21] are based on worst-case optimization. In [20], the effect of the SOI in the data covariance matrix is modeled as multi-rank for the spatially distributed source and the uncertainties for the sample covariance matrix and the SOI-only matrix are assumed to be with known uncertainty levels. The optimization problem solved in [21] has the following form:

$$\min_{\mathbf{w}} \max_{\|\boldsymbol{\Delta}_x\| \le \gamma_x} \|(\mathbf{X}+\boldsymbol{\Delta}_x)^H\mathbf{w}\| \text{ s.t. } |\mathbf{w}^H(\overline{\mathbf{a}}+\mathbf{e})| \ge 1 \ \forall \|\mathbf{e}\| \le \epsilon \tag{7}$$

where $\overline{\mathbf{a}}$ represents the nominal (or presumed) SOI steering vector, the matrix $\mathbf{X} \triangleq [\,\mathbf{x}(1) \quad \mathbf{x}(1) \quad \ldots \quad \mathbf{x}(K)\,]$ collects the received K snapshots, the error matrix $\boldsymbol{\Delta}_x$ denotes the uncertainty in the samples, and $\mathbf{e}$ stands for the uncertainty in the SOI steering vector. The notation $\|\cdot\|$ denotes the Euclidean norm. The parameters γ_x and ϵ are the preliminarily known uncertainty levels. The problem in (7) can be transferred to a second-order cone programming (SOCP) problem and thus be solved by using some existing MATLAB softwares, e.g., the CVX package [22]. The JRAB proposed in [18] combines two existing techniques in a straightforward manner. One is the so-called linear shrinkage covariance matrix estimation reported in [24] and another is an iterative method proposed in [25] in which each iteration is required to solve the following optimization problem

$$\begin{aligned} &\min_{\mathbf{e}_\perp} \ (\mathbf{a}_k + \mathbf{e}_\perp)^H \widetilde{\mathbf{R}}^{-1} (\mathbf{a}_k + \mathbf{e}_\perp) \\ &\text{s.t. } \mathbf{P}^\perp (\mathbf{a}_k + \mathbf{e}_\perp) = \mathbf{0}, \ \|(\mathbf{a}_k + \mathbf{e}_\perp)\| \le \sqrt{N} + \delta \\ &\quad \mathbf{a}_k^H \mathbf{e}_\perp = 0, \ (\mathbf{a}_k + \mathbf{e}_\perp)^H \overline{\mathbf{C}} (\mathbf{a}_k + \mathbf{e}_\perp) \le \mathbf{a}_k^H \overline{\mathbf{C}} \mathbf{a}_k \end{aligned} \tag{8}$$

where $\widetilde{\mathbf{R}}$ is estimated by the linear shrinkage estimator [24], $\mathbf{a}_k$ denotes the estimated SOI steering vector at the kth iteration, and the value of δ is preselected. The matrix $\mathbf{P}^\perp$ denotes the noise-subspace projector of the matrix $\mathbf{C} \triangleq \int_{\theta_1}^{\theta_2} \mathbf{a}(\theta)\mathbf{a}^H(\theta)d\theta$ where $[\theta_1, \theta_2]$ is the expected SOI angular range, and the matrix $\overline{\mathbf{C}} \triangleq \int_{\overline{\Theta}} \mathbf{a}(\theta)\mathbf{a}^H(\theta)d\theta$ (where $\overline{\Theta}$ denotes all the directions lying outside the sector $[\theta_1, \theta_2]$) represents the complement of $\mathbf{C}$. The optimization problem in (8) can also be rewritten as a SOCP problem and hence be solved by using the CVX toolbox [22]. However, it is worth noting that this iterative process may be time consuming since in each iteration the CVX has to be employed. The JRAB proposed in [23] is also based on worst-case optimization, in which the beamformer is formulated by the following problem

$$\min_{\mathbf{w}} \max_{\|\mathbf{\Delta}_R\| \le \gamma_R} \mathbf{w}^H \left(\widehat{\mathbf{R}} + \mathbf{\Delta}_R \right) \mathbf{w} \text{ s.t. } \mathbf{w}^H \overline{\mathbf{a}} = 1, \ \mathbf{w}^H \mathbf{Q} \mathbf{w} \le \epsilon_q \tag{9}$$

where ϵ_q is a preselected small number. The matrix $\mathbf{Q} \triangleq \int_{-\frac{\Delta_\theta}{2}}^{\frac{\Delta_\theta}{2}} [\mathbf{a}(\overline{\theta} + \phi) - \mathbf{a}(\overline{\theta})][\mathbf{a}(\overline{\theta} + \phi) - \mathbf{a}(\overline{\theta})]^H \cos\phi \, d\phi$ where Δ_θ denotes the SOI spatial sector and $\cos\phi$ is used as a weighting function. The constraint $\mathbf{w}^H\mathbf{Q}\mathbf{w} \le \epsilon_q$ in (9) aims to guarantee that the array response gain in the presumed SOI angular location does not drop sharply. Also, the JRAB proposed in [23] can be transferred to a SOCP problem and be solved by using the CVX toolbox [22].

In this paper, both the uncertainties of steering vector and covariance matrix are taken into account to develop a min–max optimization problem in which we aim to find a steering vector with the maximum output power under the worst-case covariance mismatch. Then we relax this min–max optimization problem to a max–min optimization problem which can be solved by using the Karush–Kuhn–Tucker optimality conditions. It is also shown that the proposed technique can be interpreted in terms of variable diagonal loading where the optimal loading factors are related to both the correlations (between the eigenvectors and the signal of interest) and the eigenvalues of the data covariance matrix. The remainder of this paper is organized as follows. In Sect. 2, we revisit two classical robust beamformers: the robust Capon beamformer (RCB) proposed in [17] and the signal-subspace projection method proposed in [19]. Section 3 presents the proposed variable diagonal loading beamforming. Simulations are given in Sect. 4, and conclusions are drawn in Sect. 5.

2 Problem Formulation

Let us start with the classical robust Capon beamformers (RCB) propose in [17], in which the SOI steering vector is estimated by

$$\widehat{\mathbf{a}}_{\mathrm{RCB}} = \min_{\mathbf{a}\in\mathcal{A}_1} \mathbf{a}^{\mathrm{H}}\widehat{\mathbf{R}}^{-1}\mathbf{a} \quad \text{with } \mathcal{A}_1 \triangleq \left\{\mathbf{a} \middle| \, \|\mathbf{a}-\overline{\mathbf{a}}\|^2 \le \epsilon_1\right\} \tag{10}$$

where $\overline{\mathbf{a}}$ stands for the nominal (or presumed) SOI steering vector and the preselected parameter ϵ_1 denotes the uncertainty level of the steering vector. The essence of (10) is to find a vector which, within the uncertainty set $\mathcal{A}_1$, is associated with the maximum output power [17]. The final weight vector used in [17] has a diagonal loading (DL) form as:

$$\begin{aligned}\widehat{\mathbf{w}}_{\mathrm{RCB}} &= \alpha\widehat{\mathbf{R}}^{-1}\widehat{\mathbf{a}}_{\mathrm{RCB}} \\ &= \alpha\left(\widehat{\mathbf{R}} + \xi\mathbf{I}_N\right)^{-1}\overline{\mathbf{a}} \\ &= \alpha\widehat{\mathbf{R}}^{-1}\underbrace{\left(\xi\widehat{\mathbf{R}}^{-1} + \mathbf{I}_N\right)^{-1}\overline{\mathbf{a}}}_{\triangleq\widehat{\mathbf{a}}_{\mathrm{DL}}}\end{aligned} \tag{11}$$

where the loading factor ξ can be found by solving the equation $\|(\mathbf{I}+\frac{\widehat{\mathbf{R}}}{\xi})^{-1}\overline{\mathbf{a}}\|^2 = \epsilon_1$. Performing eigen-decomposition on $\widehat{\mathbf{R}}$ yields

$$\widehat{\mathbf{R}} = \widehat{\mathbf{U}}\widehat{\boldsymbol{\Gamma}}\widehat{\mathbf{U}}^{\mathrm{H}} = \sum_{i=1}^{N}\widehat{\gamma}_i\widehat{\mathbf{e}}_i\widehat{\mathbf{e}}_i^{\mathrm{H}} \tag{12}$$

where $\widehat{\mathbf{U}} = [\,\widehat{\mathbf{e}}_1 \quad \ldots \quad \widehat{\mathbf{e}}_N\,]$ collects all the eigenvectors, and $\widehat{\boldsymbol{\Gamma}} = \mathrm{diag}\{\widehat{\gamma}_1,\ldots,\widehat{\gamma}_N\}$ is a diagonal matrix with the eigenvalues $\widehat{\gamma}_1 \ge \cdots \ge \widehat{\gamma}_N$ being nonincreasingly ordered. Thus, $\widehat{\mathbf{a}}_{\mathrm{DL}}$ defined in (11) can be rewritten as

$$\widehat{\mathbf{a}}_{\mathrm{DL}} = \sum_{i=1}^{N}\frac{\widehat{\gamma}_i}{\widehat{\gamma}_i+\xi}(\widehat{\mathbf{e}}_i^{\mathrm{H}}\overline{\mathbf{a}})\widehat{\mathbf{e}}_i \tag{13}$$

From (13), we observe that for large eigenvalues the term $\frac{\widehat{\gamma}_i}{\widehat{\gamma}_i+\xi}$ is approximately equal to one whether ξ is loaded or not. However, for small eigenvalues the term $\frac{\widehat{\gamma}_i}{\widehat{\gamma}_i+\xi}$ becomes quite small when ξ is loaded, since the loading factor ξ is positive in general. This implies that the effect of ξ is to deemphasize components corresponding to small eigenvalues.

Another robust beamformer is the signal subspace projection (SSP) method presented in [19] with the weight vector given by

$$\begin{aligned}\widehat{\mathbf{w}}_{\mathrm{SSP}} &= \alpha\widehat{\mathbf{R}}^{-1}\mathbf{P}_{\widehat{\mathbf{E}}_s}\overline{\mathbf{a}} \\ &= \alpha\widehat{\mathbf{E}}_s\mathrm{diag}\left(\left[\frac{1}{0+\widehat{\gamma}_1} \quad \cdots \quad \frac{1}{0+\widehat{\gamma}_M}\right]\right)\widehat{\mathbf{E}}_s^{\mathrm{H}}\overline{\mathbf{a}} \\ &\quad + \alpha\widehat{\mathbf{E}}_n\mathrm{diag}\left(\left[\frac{1}{\infty+\widehat{\gamma}_{M+1}} \quad \cdots \quad \frac{1}{\infty+\widehat{\gamma}_N}\right]\right)\widehat{\mathbf{E}}_n^{\mathrm{H}}\overline{\mathbf{a}}\end{aligned} \tag{14}$$

where $\mathbf{P}_{\widehat{\mathbf{E}}_s} = \widehat{\mathbf{E}}_s\widehat{\mathbf{E}}_s^{\mathrm{H}}$ is a projection operator, $\widehat{\mathbf{E}}_s = [\,\widehat{\mathbf{e}}_1 \quad \ldots \quad \widehat{\mathbf{e}}_{M+1}\,]$ and $\widehat{\mathbf{E}}_n = [\,\widehat{\mathbf{e}}_{M+2} \quad \ldots \quad \widehat{\mathbf{e}}_N\,]$, respectively, collect the eigenvectors corresponding to the signal subspace and the noise subspace. Therefore, the SSP approach uses ∞ as the loading factor to punish the noise-subspace eigenvectors and zero loading factor for the signal-subspace eigenvectors, meaning that the noise-subspace eigenvectors are discarded and nothing is done for the signal-subspace eigenvectors.

The above analysis tells us that the loading factor can be used to punish the eigenvectors associated with small eigenvalues (i.e., subdominant eigenvectors) and thus let the estimated steering vector stay away from these eigenvectors. This is reasonable because the subdominant eigenvectors often contain more noise components than signal components. However, in some practical applications, the SOI steering vector may have more correlations with some subdominant eigenvectors than the dominant eigenvectors. For instance, when the signal-to-interference ratio (SIR) is quite small, rather than the dominant eigenvectors, it is highly possible that the weak SOI is close to some eigenvectors with eigenvalues in the order of noise level. In such situation, it is unreasonable to let $\widehat{\mathbf{a}}_{\mathrm{DL}}$ approach the dominant eigenvectors since the dominant eigenvectors contain much of the strong interference signals.

3 New Robust Beamformer with Variable Diagonal Loading

The majority of the existing RCB methods consider only the steering vector uncertainty and implicitly assume that the uncertainty of the sample data covariance matrix can be incorporated into the steering vector uncertainty. However, these two kinds of uncertainties are equivalent only under the condition when both the sample size (i.e., K) and the array input signal-to-noise (SNR) are large [19]. In this paper, not only the steering vector uncertainty but the covariance matrix uncertainty are also taken into account. The optimization problem that we consider has the following form:

$$\begin{aligned} &\min_{\mathbf{a}} \max_{\boldsymbol{\Delta}} \ \mathbf{a}^{\mathrm{H}}(\widehat{\mathbf{R}} + \boldsymbol{\Delta})^{-1}\mathbf{a} \\ &\text{s.t.}\ \|\mathbf{a} - \bar{\mathbf{a}}\|^2 \leq \epsilon_1 \\ &\|\boldsymbol{\Delta}\|^2 \leq \epsilon_2. \end{aligned} \tag{15}$$

where the inner maximization corresponds to the worst array output power due to the covariance matrix uncertainty and ϵ_2 represents the uncertainty level of the covariance matrix. Equation (15) means that we would like to find a vector $\mathbf{a}$ to maximize the worst-case array output power. The global optimal solution for (15) is difficult to find. What we look for in the next, instead, is an efficient *heuristic* solution, although there is no guarantee on its optimality.

Let $\Phi(\mathbf{a}, \boldsymbol{\Delta}) = \mathbf{a}^{\mathrm{H}}(\widehat{\mathbf{R}} + \boldsymbol{\Delta})^{-1}\mathbf{a}$ denote the reciprocal of the power. Due to the weak max–min inequality (see p. 281 of [26]), we always have

$$\sup_{\boldsymbol{\Delta}} \inf_{\mathbf{a}} \Phi(\mathbf{a}, \boldsymbol{\Delta}) \leq \inf_{\mathbf{a}} \sup_{\boldsymbol{\Delta}} \Phi(\mathbf{a}, \boldsymbol{\Delta}) \tag{16}$$

which implies that $\sup_{\boldsymbol{\Delta}} \inf_{\mathbf{a}} \Phi(\mathbf{a}, \boldsymbol{\Delta})$ corresponds to an upper bound for the power. Therefore, the min–max problem in (15) can be relaxed to a max–min problem heuristically. Furthermore, we assume that the Hermitian matrix $\boldsymbol{\Delta}$ can be reparameterized as

$$\boldsymbol{\Delta} = \widehat{\mathbf{U}}\mathrm{diag}\{\beta_1, \ldots, \beta_N\}\widehat{\mathbf{U}}^{\mathrm{H}} \tag{17}$$

where $\{\beta_i\}_{i=1}^{N}$ are real numbers. Strictly speaking, it is generally not the case that the matrices $\widehat{\mathbf{R}}$ and $\boldsymbol{\Delta}$ have the same eigenvectors. However, as shown in the next, this assumption can result in a suboptimal solution which can be computed in a simple manner. Now we can transform (15) to the following problem

$$\begin{aligned} \max_{\boldsymbol{\beta}_i} \min_{\mathbf{a}} \; & \mathbf{a}^{\mathrm{H}} \widetilde{\mathbf{R}}^{-1} \mathbf{a} \\ \text{s.t.} \; & \|\mathbf{a} - \overline{\mathbf{a}}\|^2 \leq \epsilon_1 \\ & \sum_{i=1}^{N} {\beta_i}^2 \leq \epsilon_2 \end{aligned} \tag{18}$$

where $\widetilde{\mathbf{R}} = \widehat{\mathbf{R}} + \boldsymbol{\Delta} = \widehat{\mathbf{U}}\widetilde{\boldsymbol{\Gamma}}\widehat{\mathbf{U}}^{\mathrm{H}}$ and $\widetilde{\boldsymbol{\Gamma}} = \mathrm{diag}\{\widehat{\gamma}_1 + \beta_1, \ldots, \widehat{\gamma}_N + \beta_N\}$. It is clear that if $\{\beta_i\}_{i=1}^{N}$ are fixed, the minimization problem over the variable $\mathbf{a}$ is equivalent to the RCB problem in [17], implying that we can directly use the result in [17]. Hence, letting $\mathbf{z} = \widehat{\mathbf{U}}^{\mathrm{H}}\overline{\mathbf{a}}$ and z_i be the magnitude of the ith element of $\mathbf{z}$ (i.e., $z_i = |[\mathbf{z}]_i|$), the result of the minimization problem of (18) can be given by (see Eq. (30) of [17])

$$\begin{aligned} L_{\Delta} &= \overline{\mathbf{a}}^{\mathrm{H}} \widehat{\mathbf{U}} \widetilde{\boldsymbol{\Gamma}} (\lambda^{-2}\mathbf{I} + 2\lambda^{-1}\widetilde{\boldsymbol{\Gamma}} + \widetilde{\boldsymbol{\Gamma}}^2)^{-1} \widehat{\mathbf{U}}^{\mathrm{H}} \overline{\mathbf{a}} \\ &= \sum_{i=1}^{N} \frac{z_i^2(\widehat{\gamma}_i + \beta_i)}{(\widehat{\gamma}_i + \beta_i + \frac{1}{\lambda})^2} \end{aligned} \tag{19}$$

where λ satisfies

$$g(\lambda) = \sum_{i=1}^{N} \frac{z_i^2}{[1 + \lambda(\widehat{\gamma}_i + \beta_i)]^2} = \epsilon_1. \tag{20}$$

Therefore, (18) is rewritten as

$$\begin{aligned} \max_{\beta_i} \; & \sum_{i=1}^{N} \frac{z_i^2(\widehat{\gamma}_i + \beta_i)}{(\widehat{\gamma}_i + \beta_i + \frac{1}{\lambda})^2} \\ \text{s.t.} \; & \sum_{i=1}^{N} \beta_i^2 \leq \epsilon_2. \end{aligned} \tag{21}$$

Next, we will use the Karush–Kuhn–Tucker (KKT) optimality conditions to solve (21). Defining

$$f = -\sum_{i=1}^{N} \frac{z_i^2(\widehat{\gamma}_i + \beta_i)}{(\widehat{\gamma}_i + \beta_i + \frac{1}{\lambda})^2} \tag{22}$$

and modifying the objective function in (21) to minimize f, we can write the Lagrangian of that problem as

$$L = f + v\left(\sum_{j=1}^{N} \beta_j^2 - \epsilon_2\right) \tag{23}$$

where v is the Lagrange multiplier. In the "Appendix", we show that

$$\frac{\partial f}{\partial \beta_i} = \frac{\lambda^2 z_i^2}{[1 + \lambda(\widehat{\gamma}_i + \beta_i)]^2} \tag{24}$$

and therefore

$$\frac{\partial L}{\partial \beta_i} = \frac{\lambda^2 z_i^2}{[1 + \lambda(\widehat{\gamma}_i + \beta_i)]^2} + 2v\beta_i. \tag{25}$$

Hence, the complete KKT conditions can be written as [26, 27]

$$v \geq 0 \tag{26a}$$

$$v\left(\sum_{j=1}^{N} \beta_j^2 - \epsilon_2\right) = 0 \tag{26b}$$

$$\frac{\lambda^2 z_i^2}{[1 + \lambda(\widehat{\gamma}_i + \beta_i)]^2} = -2v\beta_i \; i = 1, \ldots, N \tag{26c}$$

Obviously, we know that $v > 0\,(v \neq 0)$ and $\beta_i < 0$ from (26c) as $\lambda \neq 0$ and $z_i \neq 0$. Then (26) can be recast as

$$v > 0 \tag{27a}$$

$$\sum_{j=1}^{N} \beta_j^2 = \epsilon_2 \tag{27b}$$

$$\frac{\lambda^2 z_i^2}{[1 + \lambda(\widehat{\gamma}_i + \beta_i)]^2} = -2v\beta_i, \; i = 1, \ldots, N \tag{27c}$$

Theoretically, (27) can be solved since we have $N + 2$ equations [i.e., (27b), (27c) and (20)] for $N + 2$ variables (i.e., $\{\beta_i\}_{i=1}^N$, λ and v). However, it is difficult to have closed-form solutions because (27c) is actually a cubic equation with respect to β_i. Moreover, how to choose the covariance matrix uncertainty level ϵ_2 is unclear. In order to find the loading factors in a simple way, we present the following $N + 2$ equations to replace (27):

$$\sum_{i=1}^{N} \frac{z_i^2}{[1 + \lambda(\widehat{\gamma}_i + \beta_i)]^2} = \epsilon_1 \tag{28a}$$

$$\frac{1}{\lambda} + \beta_i = \frac{z_i}{\sqrt{-2v\beta_i}} - \widehat{\gamma}_i, \; \text{for } i \neq \widetilde{m} \tag{28b}$$

$$\frac{1}{\lambda} + \beta_{\widetilde{m}} = \frac{z_m}{\sqrt{-2v\beta_{\widetilde{m}}}} - \widehat{\gamma}_{\widetilde{m}} = 0 \tag{28c}$$

where (28a) is identical to (20), (28b) is derived from (27c), and the subscript $\widetilde{m}$ in (28c) is equal to the subscript i with the maximum of $\{z_i\}_{i=1}^N$. In Sect. 2, we have shown that the loading factor does not affect the dominant eigenvectors almost in the diagonal loading methods. Inspired by this, we argue that it is reasonable to assume that the loading factor $\frac{1}{\lambda} + \beta_{\widetilde{m}}$, corresponding to the maximum of $\{z_i\}_{i=1}^N$, is equal to zero. This implies that the loading factor should not affect the eigenvector that has the maximum correlation with the SOI. Besides, another benefit offered by this reasonable assumption is that the problem of how to set the covariance matrix uncertainty level ϵ_2 is circumvented. From (28b), we can observe that the loading factor $\frac{1}{\lambda}+\beta_i$ is variable for each eigenvector. The larger eigenvalue, the less loading factor. The larger correlation (i.e., z_i), the less loading factor (or the larger absolute value of β_i).

So far, our proposed RCB approach can be presented as the following steps.

1. Perform eigen-decomposition on the estimated covariance matrix to produce $\widehat{\mathbf{R}} = \widehat{\mathbf{U}}\widehat{\boldsymbol{\Gamma}}\widehat{\mathbf{U}}^{\mathrm{H}}$ and compute $\mathbf{z} = \widehat{\mathbf{U}}^{\mathrm{H}}\overline{\mathbf{a}}$.
2. Compute the upper bound of $\frac{1}{\lambda}$ (denoted by $\left(\frac{1}{\lambda}\right)_u$) by letting all $\{\beta_i\}_{i=1}^{N}$ be equal to zero and solving (28a) (which is identical to the loading factor of the RCB in [17]) and set the lower bound $\left(\frac{1}{\lambda}\right)_l = 0$.
3. Choose $\frac{1}{\lambda} = \frac{1}{2}\left[\left(\frac{1}{\lambda}\right)_l + \left(\frac{1}{\lambda}\right)_u\right]$ and set $\beta_{\tilde{m}} = -\frac{1}{\lambda}$ to compute the variable v by using (28c).
4. Compute the rest variables β_i's by using (28b).
5. Substitute the results of $\frac{1}{\lambda}$ and $\{\beta_i\}_{i=1}^{N}$ into the left side of (28a). If the sum in the left side is greater than ϵ_1, set the upper bound $\left(\frac{1}{\lambda}\right)_u = \frac{1}{\lambda}$; otherwise, set the lower bound $\left(\frac{1}{\lambda}\right)_l = \frac{1}{\lambda}$.
6. If $\left|\left(\frac{1}{\lambda}\right)_u - \left(\frac{1}{\lambda}\right)_l\right| \le \zeta$ where ζ is a preselected threshold (say 10^{-3}), go to Step 7; otherwise, go to Step 3.
7. Construct the weight vector by

$$\widehat{\mathbf{w}} = \widehat{\mathbf{U}}\mathrm{diag}\left\{\widehat{\gamma}_1 + \beta_1 + \frac{1}{\lambda}, \ldots, \widehat{\gamma}_N + \beta_N + \frac{1}{\lambda}\right\}\widehat{\mathbf{U}}^{\mathrm{H}}\overline{\mathbf{a}}. \tag{29}$$

Although we have not proven mathematically that $g(\lambda)$ is a monotonic function of λ if the variables β_i's are considered, in the simulations we find the fact that in our proposed algorithm $g(\lambda)$ monotonically decreases with respect to λ and hence we use the bisection method to iteratively compute λ. In addition, (28b) is a cubic equation with respect to β_i and three solutions can be found for β_i. We use the following rules to choose one solution from three possible values. The first rule is that β_i is a negative real number which satisfies $\frac{1}{\lambda}+\beta_i > 0$ (since the least loading factor is $\frac{1}{\lambda}+\beta_{\tilde{m}} = 0$). The second rule is that we choose the real solution with the minimum absolute value so that we have the least covariance matrix uncertainty. If we cannot find any solution satisfying the aforementioned conditions, β_i is set to be zero, which means we choose the largest penalty for the ith eigenvector.

4 Simulation Results

Assume that one SOI and three interferers are incident on a uniform linear array with $N = 10$ isotropic sensors and half-wavelength sensor spacing. The three interference signals are from $[\theta_1, \theta_2, \theta_3] = [-10°, 10°, 50°]$ with the input interference-to-noise ratios (INRs) in a single sensor 0, 10 and 20 dB. Unless stated otherwise, the input SNR is -10 dB, the nominal direction-of-arrival (DOA) of the SOI is $\overline{\theta} = 3°$ and 50° snapshots are collected to construct the matrix $\widehat{\mathbf{R}}$. The actual SOI DOA is different and will be stated in each simulation scenario. Four other robust methods are compared with our proposed approach in terms of the array output SINR: (1) the RCB proposed in [17] where the uncertainty level ϵ_1 in (10) is equal to 5; (2) the JRAB presented by Gu [18] where the assumed SOI angular range is $[-5°, 5°]$ and the parameter δ in (8) equals to 0.1; (3) the JRAB proposed by Song [23] where $\frac{\Delta\theta}{2} = 5°$ is used to compute the matrix $\mathbf{Q}$, and $\epsilon_q =$

0.03 and $\gamma_R = 10$ are utilized; (4) the JRAB presented by Vorobyov [21] where we choose the steering vector uncertainty level $\epsilon = \sqrt{5}$ and the snapshot matrix uncertainty level $\gamma_x = \|\mathbf{X}\| \times 5\,\%$. For each scenario, the average of 200 independent runs is used to plot each simulation point. For reference, the optimal SINR is also plotted where the theoretical covariance matrix $\mathbf{R}$ and actual steering vector $\mathbf{a}_0$ are used. Note that this optimal SINR cannot be obtained in practical due to the uncertainties of the steering vector and covariance matrix.

4.1 Example 1: Look Direction Mismatch

In the first example, we consider the look direction error scenarios. We begin with comparing two RABs (both of which use only the steering vector uncertainty level ϵ_1): the RCB in [17] and our proposed method. The actual SOI DOA $\theta_0 = 0°$ is taken here (i.e., 3° look direction error). The array output SINR versus the uncertainty level ϵ_1 is plotted in Fig. 1. We can see that the proposed method maintains the output performance almost for different ϵ_1, whereas the RCB suffers if ϵ_1 is greater than 5. This means that our proposed method is less sensitive to the choice of ϵ_1 than the RCB beamformer. In the rest of our simulation scenarios, we choose $\epsilon_1 = 5$ for both robust approaches.

Figure 2 shows the performance of the five methods versus look direction error for the fixed actual DOA $\theta_0 = 0°$ and the nominal DOA $\overline{\theta}$ varying from $-5°$ to 5°. It can be seen from Fig. 2 that the proposed method outperforms other four robust methods tested within 4° look direction errors, and only JRAB of Gu [18] is better than ours when the look direction error is larger than 4°. Then we examine the effects of the snapshot number in Fig. 3 and the input SNR in Fig. 4, where the actual and nominal DOA are fixed at 0° and 3° respectively. As depicted in Figs. 3 and 4, the proposed method is also better than the other methods in terms of the array output SINR.

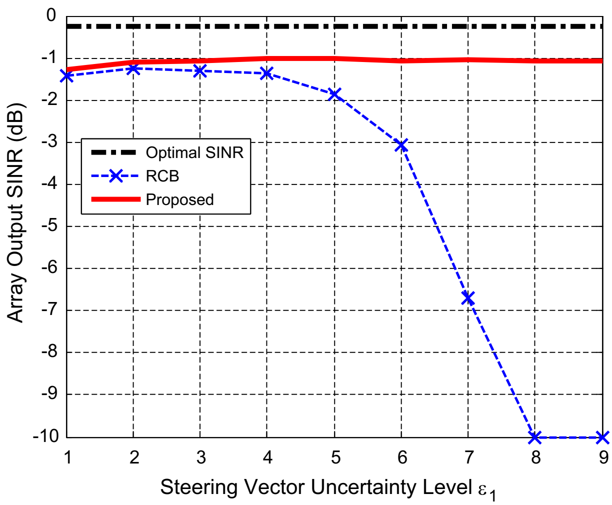

Fig. 1 Array output SINR versus steering vector uncertainty level ϵ_1; first example

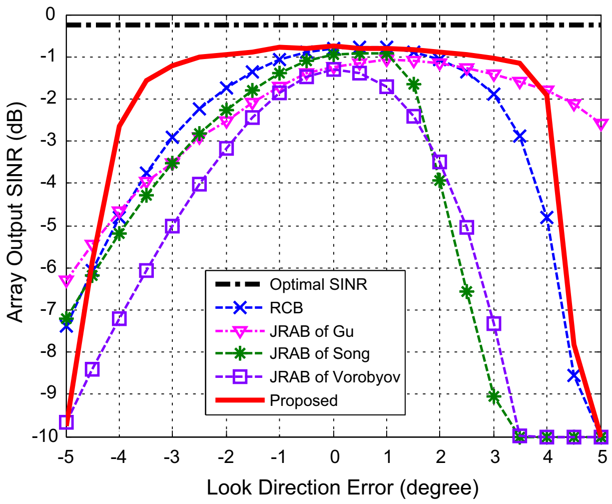

Fig. 2 Array output SINR versus look direction error; first example

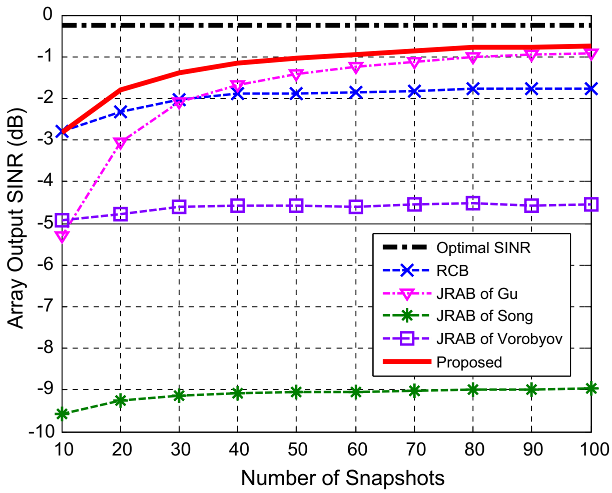

Fig. 3 Array output SINR versus snapshot number; first example

4.2 Example 2: Coherent Local Scattering

In the second example, the actual SOI steering vector is formed by five coherent signal path as [6, 20]

$$\mathbf{a} = \mathbf{a}(\theta_0) + \sum_{i=1}^{4} e^{j\phi_i} \mathbf{a}_i(\widetilde{\theta}_i) \tag{30}$$

where θ_0 is the DOA of the direct path, whereas $\widetilde{\theta}_i$ corresponds to the ith coherently scattered path. Here we assume that θ_0 and $\overline{\theta}$ are both 3°. The parameter $\{\phi_i\}$ represent the

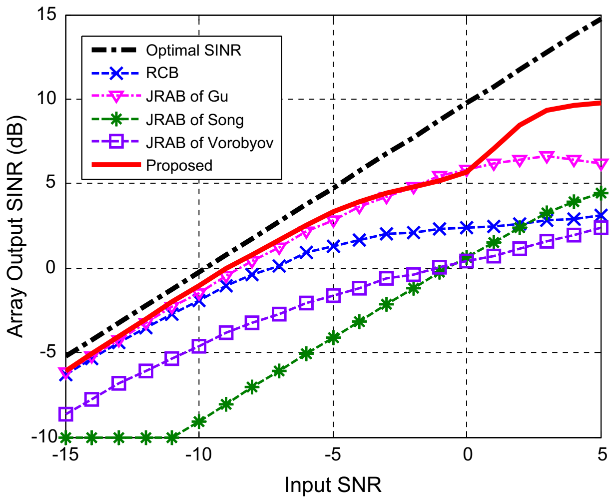

Fig. 4 Array output SINR versus input SNR; first example

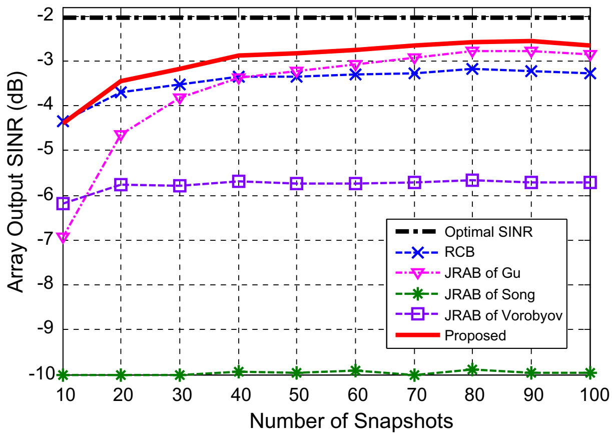

Fig. 5 Array output SINR versus snapshot number; uniform distribution; second example

path phases that are independently and uniformly drawn from the interval $[0, 2\pi]$ in each simulation run. The angles $\{\widetilde{\theta}_i\}$, $i = 1, 2, 3, 4$ are independently drawn in each simulation run from a random generator with mean equal to 3° and standard deviation (or scatter angular spread) equal to 5°. Note that $\{\widetilde{\theta}_i\}$ and $\{\phi_i\}$ vary from run to run while keeping unchanged from snapshot to snapshot.

The performances versus the snapshot number and the input SNR are displayed in Figs. 5 and 6 for the uniform distribution and in Figs. 7 and 8 for the Gaussian distribution. These four figures clearly demonstrate that our proposed robust beamformer consistently enjoys the best performance among all the tested robust approaches. In addition, the JRAB of Gu presented in [18] is another well-performing method which is comparable with ours when we examine the effect of input SNR in Figs. 4, 6 and 8. It is worthwhile to note that the JRAB of Gu must employ a process of the CVX optimization in each iteration and the

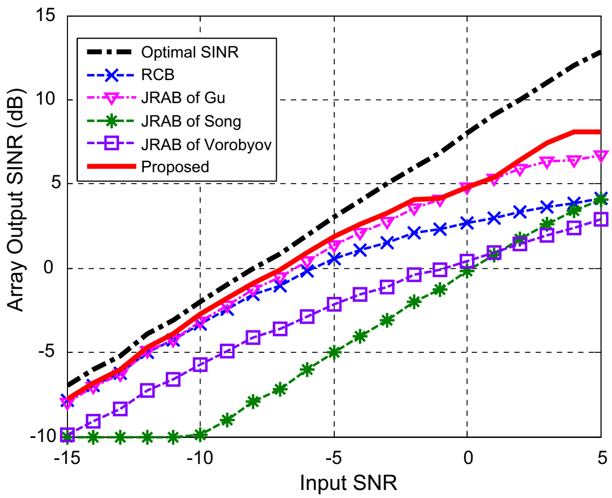

Fig. 6 Array output SINR versus input SNR; uniform distribution; second example

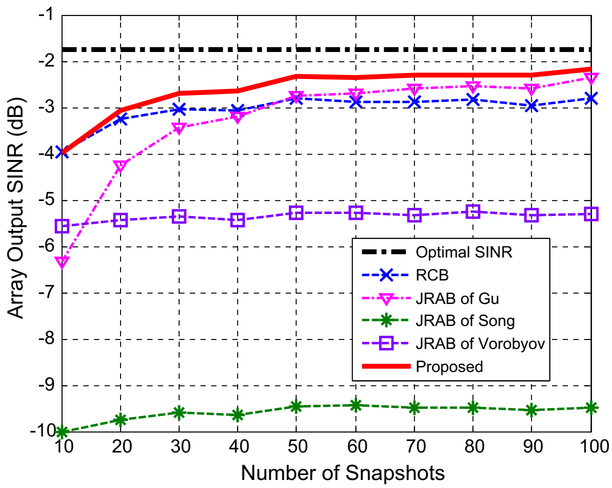

Fig. 7 Array output SINR versus snapshot number; Gaussian distribution; second example

convergence may be slow, whereas our proposed method is much more computationally effective.

5 Conclusion

Considering both the uncertainties of steering vector and covariance matrix, a min–max optimization problem is designed to find a steering vector corresponding to the maximum power under the worst covariance matrix mismatch. Such problem can be relaxed to a max–min optimization problem and then be solved by using the KKT optimality

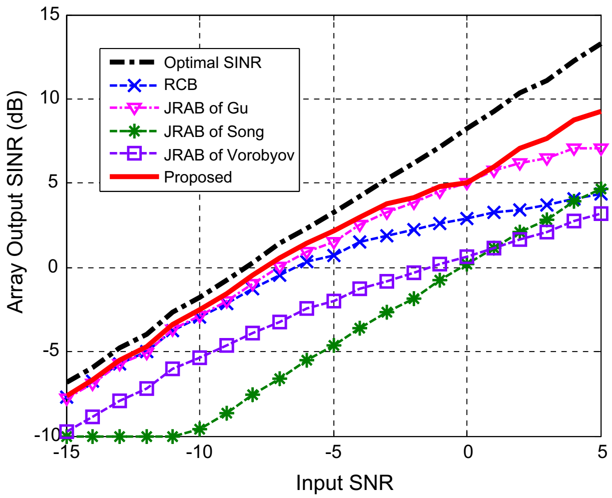

Fig. 8 Array output SINR versus input SNR; Gaussian distribution; second example

conditions. Different than the traditional DL methods, the diagonal loading factors in our proposed approach are variable and dependent on the correlations (between the eigenvectors and the SOI) and the eigenvalues.

Acknowledgments This work was supported by the open research fund of Chongqing Key Laboratory of Emergency Communications under Grant No. CQKLEC20130504, the Fundamental Research Funds for the Central Universities under Grant No. ZYGX2014J007, the Scientific Research Foundation for the Returned Overseas Chinese Scholars (SRF for ROCS, SEM) under Grant No. LXHG-47-ZJ, the National Natural Science Foundation of China under Grant No. 61301272, the Program for New Century Excellent Talents in University under Grant No. NCET-11-0873, the Program for Innovative Research Team in University of Chongqing under Grant No. KJTD201343, the Key Project of Chongqing Natural Science Foundation under Grant No. CSTC2011BA2016.

Appendix: Proof of (24)

Let us start with the equation

$$\sum_{j=1}^{N} \frac{z_j^2}{\left[1+\lambda\left(\widehat{\gamma}_j+\beta_j\right)\right]^2} = \epsilon_1. \tag{31}$$

Differentiating with respect to β_i, we have

$$\sum_{j=1}^{N} \frac{-2z_j^2\left[\left(\widehat{\gamma}_j+\beta_j\right)\frac{\partial\lambda}{\partial\beta_i}+\lambda\delta(i-j)\right]}{\left[1+\lambda\left(\widehat{\gamma}_j+\beta_j\right)\right]^3} = 0 \tag{32}$$

where $\delta(i)$ is the impulse function. Therefore,

$$\frac{\partial\lambda}{\partial\beta_i} = -\frac{\frac{\lambda z_i^2}{\left[1+\lambda\left(\widehat{\gamma}_i+\beta_i\right)\right]^3}}{\sum_{j=1}^{N}\frac{z_j^2\left(\widehat{\gamma}_j+\beta_j\right)}{\left[1+\lambda\left(\widehat{\gamma}_j+\beta_j\right)\right]^3}} \tag{33}$$

Using (22) and differentiating it with respect to β_i, we have

$$\begin{aligned}
-\frac{\partial f}{\partial \beta_i} &= \sum_{j=1}^{N} \frac{z_j^2 \delta(i-j)}{\left(\widehat{\gamma}_j + \beta_j + \frac{1}{\lambda}\right)^2} \\
&\quad + \sum_{j=1}^{N} \frac{-2 z_j^2 \left(\widehat{\gamma}_j + \beta_j\right)\left[\delta(i-j) - \frac{1}{\lambda^2}\frac{\partial \lambda}{\partial \beta_i}\right]}{\left(\widehat{\gamma}_j + \beta_j + \frac{1}{\lambda}\right)^3} \\
&= \frac{z_i^2\left[\lambda^2 - \lambda^3(\widehat{\gamma}_i + \beta_i)\right]}{\left[1 + \lambda(\widehat{\gamma}_j + \beta_j)\right]^3} + 2\lambda \frac{\partial \lambda}{\partial \beta_i} \sum_{j=1}^{N} \frac{z_j^2\left(\widehat{\gamma}_j + \beta_j\right)}{\left[1 + \lambda(\widehat{\gamma}_j + \beta_j)\right]^3}
\end{aligned} \tag{34}$$

Substituting $\frac{\partial \lambda}{\partial \beta_i}$ from (33), we have

$$\begin{aligned}
-\frac{\partial f}{\partial \beta_i} &= \frac{z_i^2\left[\lambda^2 - \lambda^3(\widehat{\gamma}_i + \beta_i)\right]}{\left[1 + \lambda(\widehat{\gamma}_i + \beta_i)\right]^3} + \frac{-2\lambda^2 z_i^2}{\left[1 + \lambda(\widehat{\gamma}_i + \beta_i)\right]^3} \\
&= -\frac{\lambda^2 z_i^2}{\left[1 + \lambda(\widehat{\gamma}_i + \beta_i)\right]^2}
\end{aligned} \tag{35}$$

which is equivalent to (24).

References

1. Gu, Y., & Leshem, A. (2012). Robust adaptive beamforming based on interference covariance matrix reconstruction and steering vector estimation. *IEEE Transactions on Signal Processing*, *60*(7), 3881–3885.
2. Li, J., & Stoica, P. (2005). *Robust adaptive beamforming*. New York: Wiley.
3. Vorobyov, S. A. (2013). Principles of minimum variance robust adaptive beamforming design. *Signal Processing*, *93*(12), 3264–3277.
4. Khabbazibasmenj, A., & Vorobyov, S. A. (2012). Robust adaptive beamforming based on steering vector estimation with as little as possible prior information. *IEEE Transactions on Signal Processing*, *60*(6), 2974–2987.
5. Landau, L., de Lamare, R. C., & Haardt, M. (2012). *Robust adaptive beamforming algorithms based on the constrained constant modulus criterion*. http://arxiv.org/abs/1310.0101.
6. Vorobyov, S. A., Gershman, A. B., & Luo, Z.-Q. (2003). Robust adaptive beamforming using worst-case performance optimization: A solution to the signal mismatch problem. *IEEE Transactions on Signal Processing*, *51*(2), 313–324.
7. Lorenz, R. G., & Boyd, S. P. (2005). Robust minimum variance beamforming. *IEEE Transactions on Signal Processing*, *53*(5), 1684–1696.
8. Chen, C.-Y., & Vaidyanathan, P. P. (2007). Quadratically constrained beamforming robust against direction-of-arrival mismatch. *IEEE Transactions on Signal Processing*, *55*(8), 4139–4150.
9. Cox, H., Zeskind, R., & Owen, M. (1987). Robust adaptive beamforming. *IEEE Transactions on Acoustics, Speech and Signal Processing*, *35*(10), 1365–1376.
10. Yu, Z.-L., Ser, W., Er, M.-H., Gu, Z., & Li, Y. (2009). Robust adaptive beamformers based on worst-case optimization and constraints on magnitude response. *IEEE Transactions on Signal Processing*, *57*(7), 2615–2628.
11. Kim, S.-J., Magnani, A., Mutapcic, A., Boyd, S. P., & Luo, Z.-Q. (2008). Robust beamforming via worst-case SINR maximization. *IEEE Transactions on Signal Processing*, *56*(4), 1539–1547.
12. Lie, J.-P., Ser, W., & See, C.-M. S. (2011). Adaptive uncertainty based iterative robust capon beamformer using steering vector mismatch estimation. *IEEE Transactions on Signal Processing*, *59*(9), 4483–4488.
13. Jin, W., Jia, W., Zhang, F., & Yao, M. (2014). A user parameter-free robust adaptive beamformer based on general linear combination in Tandem with steering vector estimation. *Wireless Personal Communications*, *75*, 1447–1462.

14. Zhuang, J., & Huang, P. (2012). Robust adaptive array beamforming with subspace steering vector uncertainties. *IEEE Signal Processing Letters*, *19*(12), 785–788.
15. Zhang, W., Wang, J., & Wu, S. (2013). Robust Capon beamforming against large DOA mismatch. *Signal Processing*, *93*(4), 804–810.
16. Zhuang, J., & Manikas, A. (2013). Interference cancellation beamforming robust to pointing errors. *IET Signal Processing*, *7*(2), 120–127.
17. Li, J., Stoica, P., & Wang, Z. S. (2003). On robust Capon beamforming and diagonal loading. *IEEE Transactions on Signal Processing*, *51*(7), 1702–1715.
18. Gu, Y. J., Zhu, W. P., & Swamy, M. N. S. (2010). Adaptive beamforming with joint robustness against covariance matrix uncertainty and signal steering vector mismatch. *Electronics Letters*, *46*(1), 86–88.
19. Feldman, D. D., & Griffiths, L. J. (1994). A projection approach to robust adaptive beamforming. *IEEE Transactions on Signal Processing*, *42*(4), 867–876.
20. Shahbazpanahi, S., Gershman, A. B., Luo, Z.-Q., & Wong, K. M. (2003). Robust adaptive beamforming for general-rank signal models. *IEEE Transactions on Signal Processing*, *51*(9), 2257–2269.
21. Vorobyov, S. A., Gershman, A. B., Luo, Z.-Q., & Ma, N. (2004). Adaptive beamforming with joint robustness against mismatched signal steering vector and interference nonstationarity. *IEEE Signal Processing Letters*, *11*(2), 108–111.
22. M. Grant, S. Boyd. (2013) CVX: Matlab software for disciplined convex programming, version 2.0 beta. http://cvxr.com/cvx.
23. Song, X., Wang, J., & Wang, B. (2010). Robust adaptive beamforming under quadratic constraint with recursive method implementation. *Wireless Personal Communications*, *53*, 555–568.
24. Du, L., Li, J., & Stoica, P. (2010). Fully automatic computation of DIagonal loading levels for robust adaptive beamforming. *IEEE Transactions on Aerospace and Electronic Systems*, *46*(1), 449–458.
25. Hassanien, A., Vorobyov, S. A., & Wong, K. M. (2008). Robust adaptive beamforming using sequential quadratic programming: An iterative solution to the mismatch problem. *IEEE Signal Processing Letters*, *15*(11), 773–736.
26. Boyd, S., & Vandenberghe, L. (2004). *Convex optimization*. Cambridge: Cambridge University Press.
27. Abdel-Samad, A., Davidson, T. N., & Gershman, A. B. (2006). Robust transmit eigen beamforming based on imperfect channel state information. *IEEE Transactions on Signal Processing*, *54*(5), 1596–1609.

Jie Zhuang is currently an Associate Professor in the School of Communication and Information Engineering at University of Electronic Science and Technology of China (UESTC). He is also with Chengdu Aerospace Communication Device Company as a Post-doctoral Fellow. He received the Ph.D. degree in electrical and electronic engineering from Imperial College London, UK, in 2011, where he was a recipient of UK/China Scholarship for Excellence Programme. His research interests lie in array signal processing, MIMO wireless communications and wearable computing.

Tao Zhang is currently with Sichuan XingBang Group Co. Ltd. He received the B.E. degree in the School of Electronic and Information engineering form Northeastern University at Qinhuangdao in 2011, and the master degree in the School of Communication and Information Engineering at University of Electronic Science and Technology of China (UESTC) in 2014, under the supervision of Dr. Jie Zhuang. His research interests lie in array signal processing and MIMO communication systems.

Jing Chen received the B.E. degree in School of Information Science and Engineering from Hunan University at 2011. He obtained the master degree in the School of Communication and Information Engineering at University of Electronic Science and Technology of China (UESTC) in 2014, under the supervision of Dr. Jie Zhuang. His research interests lie in array signal processing and MIMO communication systems.

Yulin Liu received the Ph.D degree from University of Electronic Science and Technology of China (UESTC) in 2002. From 2007 to 2008, he was a Visiting Professor at the Imperial College London, U.K. Since 2006, he has been a professor of Chongqing Communication College, Chongqing, China. Currently he is with China Electronic System Engineering Company. He has published over 100 papers in journals and conferences. His research interests include signal processing for wireless communications, compressed sensing and wireless sensor network.